JOURNAL OF SOUTHERN COMMUNICATION ENGINEERING
ISLAMIC AZAD UNIVERSITY BUSHEHR BRANCH
E-ISSN: 2980-9231
https://jce.bushehr.iau.ir
https://doi.org/10.30495/jce.2022.692365

Vol. 12/ No. 45/Autumn 2022

Research Article

Outage Performance Analysis of Multi-Antenna Full-Duplex NOMA Cellular Systems

Ahmad Memarinejad, Ph.D. Student [1] | Mohammadali Mohammadi, Associate Professor [2,3] | Mohammad Bagher Tavakoli, Assistant Professor [4]

[1]Department of Electrical Engineering, Arak Branch, Islamic Azad University, Arak, Iran, amemarinejad94@iau-arak.ac.ir

[2]Faculty of Engineering, Shahrekord University, Shahrekord 115, Iran

[3]Department of Electrical Engineering, Arak Branch, Islamic Azad University, Arak, Iran, m.a.mohammadi@sku.ac.ir

[4]Department of Electrical Engineering, Arak Branch, Islamic Azad University, Arak, Iran, m-tavakoli@iau-arak.ac.ir

Correspondence
Mohammadali Mohammadi, Associate Professor of Engineering, Shahrekord University, Shahrekord 115, Iran,
Department of Electrical Engineering, Arak Branch, Islamic Azad University, Arak, Iran, m.a.mohammadi@sku.ac.ir

Received: 9 May 2022
Revised: 13 June 2022
Accepted: 3 July 2022

Abstract

We consider a full-duplex (FD) cellular network, where uplink (UL) and downlink (DL) transmissions are performed at the same time over the same frequency band by using the non-orthogonal multiple-access (NOMA) technique. By leveraging the zero-forcing (ZF) beamforming at the FD multi-antenna base station, self-interference is mitigated, and the instantaneous sum rate of the system is maximized. More specifically, we propose two ZF-based beamforming designs at the base station, namely receive ZF (RZF) and transmit ZF (TZF) scheme, which respectively utilize the receive and transmit antennas at the BS to cancel out the SI at the BS. We derive closed-form expression for the outage probability of the NOMA near and far users as a function of different system parameters. Finally, we examine the accuracy of the results by using extensive simulation results. Our numerical results show that for both TZF and RZF scheme, increasing the number of transmit and receive antenna is beneficial to improve the outage performance of the DL near user, while increasing the number of transmit and receive antenna significantly improve the outage performance of the DL far user with RZF scheme.

Keywords: Non-Orthogonal Multiple Access (NOMA), Full-Duplex (FD), Beamforming, Outage Probability

Highlights

- Integrating non-orthogonal multiple–access (NOMA) and full-duplex (FD) communication into cellular systems
- Enhancing the spectral efficiency of the cellular systems
- Applying zero-forcing based beamforming at the FD base station and deriving the outage probability performance of NOMA uplink and downlink users

Citation: A. Memarinejad, M. Mohammadi, and M. B. Tavakoli, "Outage Performance Analysis of Multi-Antenna Full-Duplex NOMA Cellular Systems," *Journal of Southern Communication Engineering*, vol. 12, no. 45, pp. 1–18, 2022, doi:10.30495/jce.2022.692365.

1. Introduction

The ever-increasing number of mobile users along with the escalating demands for the ubiquitous coverage in the future wireless networks, has led to emerging new technologies to enhance the spectral efficiency. Among them, full-duplex (FD) communications and non-orthogonal multiple access (NOMA) are primary ones to fulfill the requirement and goals setup of the future beyond fifth generation (B5G) wireless networks [1]-[4]. Individually, each technology has its own unique points and characteristics. More importantly, these two technologies complement each other when integrated together and can achieve higher performance gains compared to their individual performances. FD communications, which relies on simultaneous transmitting and reception over the same frequency band, can potentially double the spectral efficiency of traditional half-duplex (HD) systems [4]. However, the main challenge hindering the implementation of practical FD radios is the self-interference (SI), caused by signal leakage from transceiver output to its input. Thanks to recent advances in antenna and transceiver design [5], the FD radios are becoming feasible reality and thus are widely deploying in different wireless networks such as cellular networks [6], cooperative networks [7], and cognitive radio networks [8]. On the parallel avenue, NOMA also offers superior spectral efficiency over traditional orthogonal multiple access (OMA) techniques [9]. NOMA performs non-orthogonal resource allocation among multiple users at the expense of increased signal processing and receiver complexity [9]. NOMA is broadly classified into power-domain NOMA and code-domain NOMA. More specifically, in power-domain NOMA, which is the focus of this paper, users are multiplexed in the power domain by assigning distinct power levels to different users. Users with less power allocated will use the successive interference cancellation (SIC) to decode their own messages by first removing the other user's information from their received signal. On the other hand, users with more power allocated decode their own messages by treating the other users' information as noise.

Recently, the coexistence of NOMA and FD to efficiently improve the spectral efficiency of wireless networks has been analytically and numerically studied in [10]-[11]. The authors of [12] show that the FD cooperative NOMA system can improve the ergodic sum-rate in comparison to HD cooperative NOMA system at low-to-moderate signal-to-noise ratio (SNR) region. In [13], the authors studied the performance of a FD cooperative network, where a transmitter communicates with two NOMA users via one node selected from a set of FD relays. The authors of [14] proposed joint optimum beamforming design and power allocation problem to maximize the achievable rate of FD relay assisted cognitive radio NOMA systems. In order to sufficiently utilize both idle and underutilized spectrum resources, an FD cooperative NOMA scheme based on spectrum sensing for an UL relaying system has been proposed in [15], where a primary user uploads messages to the base station (BS) with the assistance of a secondary user. In [16], the authors investigated the problem of joint user association and power allocation to maximize the overall system's spectral efficiency, subject to user-specific quality-of-service (QoS) and total transmit power constraints. In [17], a joint subcarrier and power allocation algorithm was proposed to maximize the weighted sum throughput of multiuser FD NOMA systems. The work in [18] has considered DL NOMA transmission between an access point and two groups of NOMA users, where far users are aided by FD multi-antenna relays. The feasibility of FD-NOMA in single-antenna cellular networks, where UL and DL NOMA transmissions are carried out at the same time has been studied in [21]. In our recent work [22], we extended the work in [23] to the FD-NOMA cellular networks with multi-antenna BS and studied the achievable rates and performance gains achieved by deploying multi-antenna at the BS. However, the proposed beamforming design in [bb] entails high computational complexity at the FD BS. In order to provide a trade-off between the complexity and performance, in this paper, we investigate the performance of the multi-antenna FD-NOMA cellular networks with zero-forcing (ZF)-based beamforming designs at the BS. More specifically, we consider an FD NOMA-based cellular system, where a multi-antenna FD BS simultaneously communicates with multiple HD UL and DL users. The multiple antenna at the BS allows to investigate the NOMA performance with different beamforming designs and achieve spatial domain SI suppression at the FD BS. We assume that during each time slot, the BS communicates with two UL users and two DL users over the same frequency band using NOMA. Two ZF-based beamforming schemes, namely receive ZF (RZF) and transmit ZF (TZF) scheme, are proposed to completely cancel the SI at the BS and enhancing the outage performance of the NOMA users. More specifically, RZF (TZF) scheme utilize the receive (transmit) antennas at the BS to cancel out the SI at the BS. Then, we derive closed-form expressions for the outage probability of the NOMA near and far users as a function of the different system parameters. Our findings show that by using RZF beamforming scheme the outage performance of the far DL user can be significantly improved.

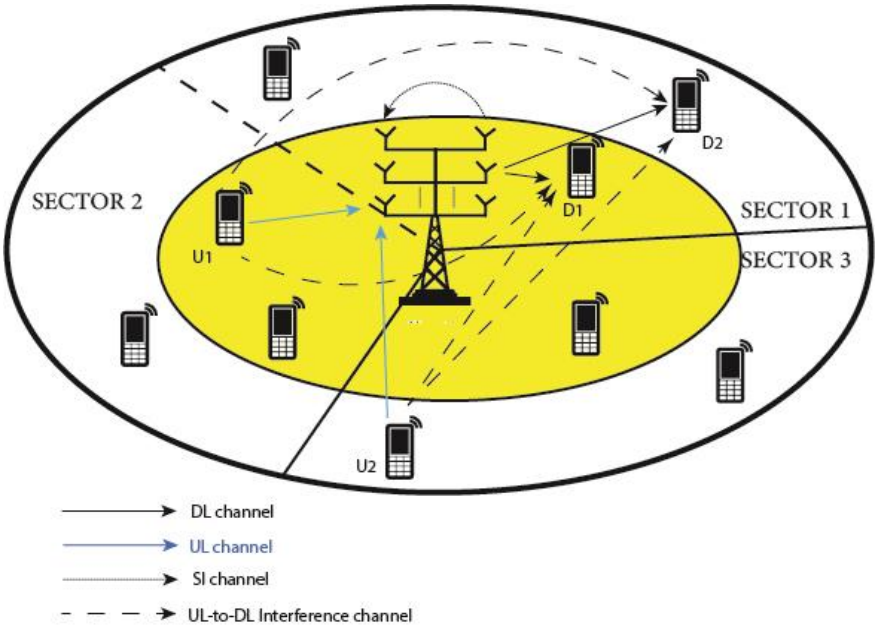

Figure 1. NOMA system model with FD BS

2. System Model

We consider a single-cell cellular system, consisting of a single multi-antenna BS, DL NOMA users and UL NOMA users. All users are in a circular area with radius R and the BS is located at the cell center. All users are equipped with single antenna and operate in HD mode, while the FD BS is equipped with M antennas of which N_{rx} antennas are dedicated to serve UL users and N_{tx} antennas are used to serve DL users. We assume that the coverage area of the BS is divided into three sectors. Moreover, each sector is split into two zones, inner and outer zones, as illustrated in Fig. 1. To apply the NOMA concept, one UL (DL) user from the inner zone and another UL (DL) user from the outer zone are selected. As a distance-based channel model is adopted in this paper, the inner zone S_1(of radius R_1) is introduced to model the minimum propagation path loss in the empirical path loss model, while the outer radius S_2(of radius R_2) denotes the cell size [18], [19], [20], as illustrated in Fig. 1. In particular, one DL user within S_1 and another DL user within S_2 of the same sector, with the shortest and farthest distance from BS are respectively selected. From the remaining two sectors, two UL users, one user within $S_1$and one user within S_2, with nearest and furthest distance to the BS are respectively scheduled. To avoid/reduce the interference from the UL interferer to the DL user, we introduce the strong interference region which is centered at the DL user with radius R_i. The UL user located within the region is deemed as strong interferer while the UL user located outside the region is deemed as weak interferer. Therefore, UL users (with nearest and furthest distance to the BS) are selected among those UL users located outside the interference region of the selected DL users. Therefore, one pair of NOMA UL user and one pair of NOMA DL users are formed, and data from users in the UL channel, and data to the users in the DL channel are transmitted and received at the same time on the same frequency. The sets of UL and DL users are denoted by $K_{ul} = \{U_i\}_{i=1:k_{ul}}$ and $K_{dl} = \{D_i\}_{i=1:k_{dl}}$, respectively, where $|kul| = kul$ and $|kdl| = kdl$.

2-1 Transmission Protocol and Signaling

We assume that data transmission is performed on a slot-by slot basis, where all time slots have equal length. For a given time slot, the BS serves a pair of DL users, D_1 (termed as NOMA near DL user) and D_2 (termed as NOMA far DL user), by applying the NOMA concept. At the same time, the BS applies NOMA concept and receives the information sent by a pair of selected UL users, U_1 (termed as NOMA near UL user) and U_2 (termed as NOMA far UL user). Therefore, the DL reception at the users are subjected to interference from the simultaneous transmissions of the UL user, while the UL reception at the FD BS is impaired by the SI. According to the NOMA concept, the BS transmits the superimposed signal intended for the NOMA DL users as

$$s[n] = \sqrt{P_b a_1}\, x_{dl,1}[n] + \sqrt{P_b a_2}\, x_{dl,2}[n] \tag{1}$$

where P_b is the BS transmit power, $x_{dl,k}, k \in \{1,2\}$ is the signal intended for D_k, a_i denotes the NOMA power allocation coefficient, such that $a_1 + a_2 = 1$ and $a_1 < a_2$ [2]. Since UL and DL transmissions take place in the same time-frequency resource, the UL signals interfere with the receive signal at the DL users. Hence, the received signal at the $k-th$ DL user can be expressed as

$$y_k[n] = \boldsymbol{h}_{dl,k}\boldsymbol{w}_t s[n] + \sum_{j=1}^{2}\sqrt{P_j}h_{jk}x_{ul,j}[n] + n_k[n] \quad (2)$$

where $\boldsymbol{h}_{dl,k} \in C^{1\times N_{tx}}$ denotes the channel vector between the BS and DL user k and its entries are identically independent distributed (i.i.d) $CN(0,\beta_{dl,k})$, $\boldsymbol{w}_t \in C^{(N_{tx}\times 1)}$ is the precoding vector at the BS, and $n_k[n]$ denotes the Additive White Gaussian noise (AWGN) at the receiver of DL user k. In (2), the second term presents the UL-to-DL CCI, where $\boldsymbol{h}_{jk}$ denotes the channel between $j-th$ UL user and $k-th$ DL user, P_j and $x_{ul,j}[n]$ are the transmit power and transmit signal from the $j-th$ UL user, respectively. D_1 performs the SIC to cancel the signal intended for D_2. Therefore, according to the SIC concept, D_1 detects the signal intended for D_2 and subtract the relevant component from the received signal. Accordingly, the achievable rate of D_1 to detect D_2 signal, i.e., $R_{2\to1}^{dl}$, and the achievable rate of D_2, i.e., R_2^{dl}, can be expressed as

$$R_{2\to1}^{dl} = \log\left(1 + \frac{p_b a_2 \left|\boldsymbol{h}_{dl,1}\boldsymbol{w}_t\right|^2}{p_b a_1 \left|\boldsymbol{h}_{dl,1}\boldsymbol{w}_t\right|^2 + I_{dl,1} + \sigma_n^2}\right) \quad (3)$$

$$R_2^{dl} = \log\left(1 + \frac{p_b a_2 \left|\boldsymbol{h}_{dl,2}\boldsymbol{w}_t\right|^2}{p_b a_1 \left|\boldsymbol{h}_{dl,2}\boldsymbol{w}_t\right|^2 + I_{dl,2} + \sigma_n^2}\right) \quad (4)$$

where $I_{dl,1} = \sum_{j=1}^{2}\rho_j\left|h_{j1}\right|^2$ and $I_{dl,2} = \sum_{j=1}^{2}\rho_j\left|h_{j2}\right|^2$ are the UL-to-DL CCI at D_1 and D_2 respectively. To ensure the SIC decoding $R_{2\to1}^{dl} > \gamma_2$ must be satisfied [22], where γ_2 denotes targeted data rate for D_2. Accordingly, D_1performs SIC and cancels the CCI from D_2. Hence, the achievable rate of the DL near user can be expressed as

$$R_1^{dl} = \log\left(1 + \frac{p_b a_1 \left|\boldsymbol{h}_{dl,1}\boldsymbol{w}_t\right|^2}{I_{dl,1} + \sigma_n^2}\right) \quad (5)$$

2-2 Uplink Transmission

In the UL, the BS receives signals from the pair of UL NOMA users. Specifically, the received signal from scheduled UL users at the BS can be written as

$$\mathrm{r_k}[\mathrm{n}] = \mathbf{w}_\mathrm{r}\sum_{\mathrm{j=1}}^{2}\sqrt{\rho_\mathrm{j}}\mathbf{h}_{\mathrm{ul,j}}\mathrm{x}_{\mathrm{ul,j}}[\mathrm{n}] + \mathbf{w}_\mathrm{r}\mathbf{H}_{\mathrm{SI}}\mathbf{w}_\mathrm{t}\mathrm{s}[\mathrm{n}-\tau] + \mathbf{w}_\mathrm{r}\mathbf{n}_\mathrm{B}[\mathrm{n}] \quad (6)$$

where $w_r \in C^{1\times N_{rx}}$ denotes the receive combining vector at the BS, $\boldsymbol{h}_{ul,j} \in C^{N_{rx}\times 1}$ is the channel between the $j-th$ UL user and BS, which its entries are i.i.d, $CN(0,\beta_{ul,k})$, τ is the processing delay due to the FD operation at the BS [12], and $\boldsymbol{n_B}$ is the AWGN vector at the BS. We model the $N_{rx}\times N_{tx}$ SI channel with Rayleigh flat fading which is a well-accepted model in the literature [4]-[5]. In this model, the strong line-of-sight component of the SI channel is cancelled and removed during the SI cancellation process employed at the BS. Therefore, the residual interference is mainly affected by the Rayleigh fading component of the loopback channel and its strength is proportional to the level of suppression achieved by the adopted specific cancellation method. Since each implementation of a particular analog/digital SI cancellation scheme can be characterized by a specific residual power, the elements of $\boldsymbol{H}_{SI}$ can be modeled as i.i.d. $CN(0,\delta_{SI}^2)$ RVs.

The BS employs SIC receiver to separate the received overlapped signals form the UL users. Consider a general M-user UL NOMA system, where M UL users simultaneously transmit to a common BS over the same frequency

band. The superimposed signal of M users is received at the BS. Since the received signal from the UL user with strongest channel is likely the strongest at the BS, the BS decodes this signal first. In this way, this user experiences interference from all other UL users. Then, the BS subtracts this signal from the received superimposed signal and then the signal for the second highest channel gain user is decoded and so on. Therefore, the user with best channel condition experiences interference from all users and the user with worst channel condition enjoys interference-free transmission [24]-[25]. That is, before BS detects the $k-th$ UL user's signal, it decodes the prior $i-th$ UL user's signal first, then removes the signal from its observation, in a sequential way. Accordingly, the achievable rate of the $k-th$ UL user is given by

$$R_k^{ul} = \log\left(1+\frac{p_k\left|\boldsymbol{w}_r\boldsymbol{h}_{ul.k}\right|^2}{\sum_{j=k+1}^{2}p_j\left|\boldsymbol{w}_r\boldsymbol{h}_{ul.j}\right|^2+p_b\left|\boldsymbol{w}_r\boldsymbol{H}_{SI}\boldsymbol{w}_t\right|^2+\sigma_n^2}\right), k=1,2 \tag{7}$$

3. Beamforming Design

The achievable UL and DL rates in (4), (5), and (7) depend on the receive and transmit beamforming vectors at the BS. These two beamforming vectors can be jointly designed at the BS to provide the UL and DL system requirements. In our recent work [12], we proposed a joint beamforming design at the BS to maximize the system DL sum-rate, under QoS constraints for the UL users. In this section, we first present the results for joint beamforming design from [13]. To provide a trade-off between the complexity and performance, we then propose ZF-based beamforming designs to cancel the SI at the BS, while improving the achievable DL/UL rates. For all beamforming design, similar to [10], we assume that the perfect knowledge of the channel side information (CSI) for every channel is known at the BS. However, such an assumption is optimistic because of the presence of channel estimation errors, time-variations of the channel and outdated CSI values [26]. Therefore, it will be interesting to investigate the implication of channel estimation errors on the system performance. However, it is still interesting to design the transmit and receive beamforming vectors assuming perfect CSI since it will present the highest possible theoretical upper bound.

3-1 Optimum Beamforming Design

DL beamformer $\boldsymbol{w_t}$ and UL beamformer $\boldsymbol{w_r}$ can be jointly designed to maximize the system DL sum-rate, under QoS constraints for the UL users. It is worth mentioning that, unlike conventional HD cellular NOMA systems for which the DL beamforming as well as the UL beamforming problem can be separately solved, the DL and UL transmission strategies must be jointly optimized in the FD cellular systems due to the coexistence of UL and DL communications and new interference sources in the FD cellular networks. Therefore, the optimization problem can be formulated as follows:

$$\boldsymbol{P}_1: \quad \max_{\mathbf{w}_r\mathbf{w}_t}\log\left(1+\frac{\mathrm{P_b a_1}\left|\mathbf{h}_{\mathrm{dl},1}\mathbf{w}_t\right|^2}{\mathrm{I}_{\mathrm{dl},1}+\sigma_n^2}\right)+\log\left(1+\frac{\mathrm{P_b a_2}\left|\mathbf{h}_{\mathrm{dl},2}\mathbf{w}_t\right|^2}{\mathrm{p_b a_1}\left|\mathbf{h}_{\mathrm{dl},2}\mathbf{w}_t\right|^2+\mathrm{I}_{\mathrm{dl},2}+\sigma_n^2}\right) \tag{7a}$$

$$s.t \quad \log\left(1+\frac{\mathrm{P}_1\left|\mathbf{w}_r\mathbf{h}_{\mathrm{ul},1}\right|^2}{\mathrm{P}_2\left|\mathbf{w}_r\mathbf{h}_{\mathrm{ul},2}\right|^2+\mathrm{P_b}\left|\mathbf{w}_r\mathbf{H}_{\mathrm{SI}}\mathbf{w}_t\right|^2+\sigma_n^2}\right)\geq\gamma_1 \tag{7b}$$

$$\log\left(1+\frac{P_2\left|\boldsymbol{w}_r\boldsymbol{h}_{ul,2}\right|^2}{P_b\left|\boldsymbol{w}_r\boldsymbol{H}_{SI}\boldsymbol{w}_t\right|^2+\sigma_n^2}\right)\geq\gamma_2 \tag{7c}$$

$$\log\left(1+\frac{\mathrm{P_b a_2}\left|\mathbf{h}_{\mathrm{dl},1}\mathbf{w}_t\right|^2}{\mathrm{P_b a_1}\left|\mathbf{h}_{\mathrm{dl},1}\mathbf{w}_t\right|^2+\mathrm{I}_{\mathrm{dl},1}+\sigma_n^2}\right)>\gamma_2 \tag{7d}$$

$$\boldsymbol{w}_t=1\ ,\ \boldsymbol{w}_r=1$$

where the constraint (7c), guarantees the feasibility of SIC at D_1. The optimization problem (7) is a complicated non-convex problem and difficult to solve. The key observation is that, when the UL beamformer $\boldsymbol{w}_r$ is fixed, problem (7) can be recast as a convex problem. Therefore, utilizing the alternative optimization (AO) algorithm [12], which is used for multivariate optimization in an alternating manner, Problem ($\boldsymbol{P_1}$) can be solved. More specifically, we first optimize $\boldsymbol{w}_t$ given $\boldsymbol{w}_r$, and then optimize $\boldsymbol{w}_r$ given $\boldsymbol{w}_t$, which is performed alternatively in an iterative manner to obtain the target values of $\boldsymbol{w}_t$ and $\boldsymbol{w}_r$ [12]. In other words, to implement the AO process, we update the transmit beamformer after each update of receive beamformer. If this iterative process converges, it converges to a fixed point, which is also a stationary point of the objective function [25]. The AO algorithm to jointly optimize the transmit and receive beamformers at the BS is presented in Table. I from [12], where $\boldsymbol{A}_1 = \boldsymbol{I}_{Ntx} + \frac{P_b a_1}{I_{dl.1}+\sigma_n^2}\boldsymbol{H}_{dl.1}$, $\boldsymbol{B}_1 = (I_{dl.1} + \sigma_n^2)\boldsymbol{I}_{Ntx} + P_b\boldsymbol{H}_{dl.2}$, $\boldsymbol{B}_2 = (I_{dl.1} + \sigma_n^2)\boldsymbol{I}_{Ntx} + P_b a_1\boldsymbol{H}_{dl.2}$, $\boldsymbol{C}_1 = (I_{dl.1} + \sigma_n^2)\boldsymbol{I}_{Ntx} + P_b a_1\boldsymbol{H}_{dl.1}$, $\boldsymbol{D_1} = \boldsymbol{H}_{S_1}^{+}\boldsymbol{W}_r\boldsymbol{H}_{SI}$, with $\boldsymbol{W}_r = \boldsymbol{w}_r^{+}\boldsymbol{w}_r$, $\boldsymbol{H}_{dl.1} = \boldsymbol{h}_{dl}^{+}\boldsymbol{h}_{dl.1}$, $\boldsymbol{H}_{dl.2} = \boldsymbol{h}_{dl.2}^{+}\boldsymbol{h}_{dl.2}$.
two optimization problem ($\boldsymbol{P}_2$) and ($\boldsymbol{P}_3$) are solved. by defining the slack variable $t_1 = \frac{\boldsymbol{w}_t^{+}\boldsymbol{B_1}\boldsymbol{w_t}}{\boldsymbol{w}_t^{+}\boldsymbol{B_2}\boldsymbol{w_t}} \geq 0$, the optimization problem $\boldsymbol{P_2}$ to find the optimum transmit ($\boldsymbol{w}_t$) is given as [20]

$$\boldsymbol{P}_2: \quad \max_{\boldsymbol{W}_t, t_1 \geq 0} \quad tr\left(\boldsymbol{A}_1\boldsymbol{W}_t\right).t_1 \tag{8a}$$

$$St. \quad tr\left(\boldsymbol{B}_1 - t_1\boldsymbol{B}_2\right)\boldsymbol{W}_t \geq 0 \tag{8b}$$

$$tr\left(\left(\boldsymbol{H}_{dl.1} - \frac{v_2}{P_b a_2}\boldsymbol{C}_1\right)\boldsymbol{W}_t\right) \geq 0 \tag{8c}$$

Moreover, at each iteration of ***Algorithm 1***

Algorithm 1. AO algorithm based on SDR to find $\boldsymbol{w_t}$ and $\boldsymbol{w}_r$ for Problem $\boldsymbol{P_1}$ **[20]**

Step 1: 1: Initialize $\boldsymbol{w}_r$ as $\boldsymbol{w}_r^0$, and $t_1 = \lambda_{min}(\boldsymbol{B}_2^{-1}\boldsymbol{B}_1)$

2: Initialize the iteration number $n = 1$

2: Set $G_0 = 0$. Given maximum tolerance error ε_1

Step 2:

Given $\boldsymbol{w}_r$ as $\boldsymbol{w}_r^{n-1}$, solve Problem $\boldsymbol{P_2}$ to obtain optimal solution $\boldsymbol{w}_t^*$.

Update $\boldsymbol{w}_t^n = \boldsymbol{w}_t^*$.

Given $\boldsymbol{w}_t$ as $\boldsymbol{w}_t^n$, solve Problem $\boldsymbol{P_3}$ to obtain optimal solution $\boldsymbol{w}_r^*$.

Update $\boldsymbol{w}_r^n = \boldsymbol{w}_r^*$.

Gn = tr($\boldsymbol{A}_1\boldsymbol{w}_t^n$)

until $|G_n - G_{n-1}| \leqslant \varepsilon 1$

Step 2: Take $\boldsymbol{w}_t$ and $\boldsymbol{w}_r$.

$$tr\left(\boldsymbol{D}_1\boldsymbol{W}_t\right) \leq min\left(\frac{P_1\left|\boldsymbol{w}_r\boldsymbol{h}_{ul.1}\right|^2}{P_b v_1} - \frac{P_2}{P_b}\left|\boldsymbol{w}_r\boldsymbol{h}_{ul.2}\right|^2 . \frac{P_2\left|\boldsymbol{w}_r\boldsymbol{h}_{ul.2}\right|^2}{P_b v_2}\right) - \frac{\delta_n^2}{P_b} \tag{8d}$$

$$tr\left(\boldsymbol{W}_t\right) = 1 \tag{8e}$$

$$\boldsymbol{W}_t \geq 0 \quad .t_1 \geq 0 \tag{8f}$$

The optimal solution to the problem $\boldsymbol{P_2}$ can be found by one dimensional search over t_1 where in each iteration an SDP is solved. Therefore, we need to find the upper and lower bounds of slack variable t_1. Since t_1 has the Rayleigh quotient form, the upper and lower bound on t_1 are given by

$$\lambda_{min}\left(\boldsymbol{B}_2^{-1}\boldsymbol{B}_1\right) \le t_1 \le \lambda_{max}\left(\boldsymbol{B}_2^{-1}\boldsymbol{B}_1\right) \tag{9}$$

The optimization problem $\boldsymbol{P_3}$ to find the optimum receive ($\boldsymbol{w}_r$) beamforming vector is given by [22]

$$\boldsymbol{P}_3: \quad Find \quad \boldsymbol{W}_r \tag{10a}$$

$$S.t \quad \frac{tr\left(\boldsymbol{H}_{ul.1}\boldsymbol{W}_r\right)}{tr\left(\boldsymbol{E}_1\boldsymbol{W}_r\right)} \ge \frac{v_1}{P_1} \tag{10b}$$

$$\frac{tr\left(\boldsymbol{H}_{ul.2}\boldsymbol{W}_r\right)}{tr\left(\boldsymbol{E}_2\boldsymbol{W}_r\right)} \ge \frac{v_2}{P_2} \tag{10c}$$

$$\boldsymbol{W}_r \ge 0 \tag{10d}$$

The complexity of solving the SDR Problem $\boldsymbol{P_2}$ is O($N_{tx}^{4.5}$) [28]. Moreover, since one-dimensional optimization along t_1 is required, Problem $\boldsymbol{P_2}$ needs to be solved T_1 times, where T_1 is the number of quantization point on t_1. Therefore, the total running time is O($T_1 N_{tx}^{4.5}$). Moreover, the running time of the SDR Problem $\boldsymbol{P_3}$ is O($N_{rx}^{4.5}$). Therefore, the computation complexity of the proposed ***Algorithm 1*** is $O(T_1 N_{tx}^{4.5} + N_{rx}^{4.5})$.

3-2 ZF Beamforming

The proposed optimum beamforming design entails high computational complexity, especially when the number of transmit and receive antennas are large. Therefore, in this subsection we propose two sub-optimal beamforming designs relying on the ZF principle [27]. By deploying ZF-based beamforming schemes, FD BS takes advantage of multiple receive/transmit antennas to completely cancel the SI, while the computational complexity of the system is significantly decreased.

3-2-1 TZF Scheme

With TZF beamforming scheme, the BS take advantage of multiple transmit antenna to completely cancel the SI. Therefore, to implement the TZF scheme the number of transmit antennas at BS must be greater than one, i.e., $N_{tx} > 1$. We apply MRC at the receive side of the BS, i.e., $\boldsymbol{w}_r^{MRC} = \frac{\boldsymbol{h}_{ul,1}}{\|\boldsymbol{h}_{ul,1}\|}$, to maximize the UL achievable rate at the BS. Accordingly, the optimum transmit beamforming vector $\boldsymbol{w_t}$ is obtained by solving the following optimization problem

$$\begin{aligned} &\max_{\boldsymbol{w}_t=1} \left|\boldsymbol{h}_{dl,1}\boldsymbol{w}_t\right|^2 \\ &s.t \quad \boldsymbol{w}_r\boldsymbol{H}_{SI}\boldsymbol{w}_t = 0 \end{aligned} \tag{11}$$

Therefore, for given $\boldsymbol{w}_r^{MRC}$, the optimum transmit beamforming vector cancel the SI at the BS. By using similar steps as in [7], the optional transmit beamforming vector is obtained as

$$\boldsymbol{w}_t^{ZF} = \frac{\boldsymbol{B}\boldsymbol{h}_{dl,1}^{+}}{\boldsymbol{B}\boldsymbol{h}_{dl.1}^{+}} \tag{12}$$

where $\boldsymbol{B} = \boldsymbol{I}_{N_{tx}} - \frac{\boldsymbol{H}_{SI}^{+}\boldsymbol{h}_{ul.}\boldsymbol{h}_{ul.1}^{+}\boldsymbol{H}_{SI}}{\left\|\boldsymbol{h}_{ul.k}^{+}\boldsymbol{H}_{SI}\right\|^2}$. To this end, by substituting $\boldsymbol{w}_t^{ZF}$ and $\boldsymbol{w}_r^{MRC}$ into (1) and (2), the achievable UL rate of the NOMA near and far user can be expressed as

$$\boldsymbol{R}_1^{ul} = \log_2\left(1+\frac{P_1\boldsymbol{w}_r^{MRC}\boldsymbol{h}_{ul.1}{}^2}{p_2\left|\boldsymbol{w}_r^{MRC}\boldsymbol{h}_{ul.2}\right|^2+\sigma_n^2}\right) = \log_2\left(1+\frac{p_1 y_1}{p_2 y_2+\sigma_n^2}\right) \tag{13}$$

$$\boldsymbol{R}_2^{ul} = \log_2\left(1+\frac{p_2\left|\boldsymbol{w}_r^{MRC}\boldsymbol{h}_{ul.2}\right|^2}{\sigma_n^2}\right) = \log_2\left(1+\frac{p_2 y_2}{\sigma_n^2}\right) \tag{14}$$

respectively, where $y_1 = \|\boldsymbol{w}_r^{MRC}\boldsymbol{h}_{ul.1}\|^2$ is a Chi-squared RV with 2 N_{tx} degrees-of-freedom which is denoted by $y_1 \sim x^2_{2Ntx}$. Moreover, $y_2 = |\boldsymbol{w}_r^{MRC}\boldsymbol{h}_{ul.2}|^2$, which is an exponential RV [7], denoted by $y_2 \sim exp(\lambda_{ul,2})$.

3-2-2 RZF Scheme

As an alternative beamforming solution, the transmit beamforming vector is designed according to MRT principle, i.e., $\boldsymbol{w}_t^{MRT} = \frac{\boldsymbol{h}_{dl,1}^{\dagger}}{\|\boldsymbol{h}_{dl,1}\|}$. Moreover, the receive beamforming vector $\boldsymbol{w}_r$ is designed to cancel the SI, i.e., $\boldsymbol{w}_r\boldsymbol{H}_{SI}\boldsymbol{w}_t = 0$, to make this possible, the number of receive antennas at BS must be greater than one, i.e., $N_{rx} > 1$. In other words, the optimal receive beamforming vector is the solution of the following optimization problem:

$$\begin{aligned} &\max_{\boldsymbol{w}_r=1}\left|\boldsymbol{w}_r\boldsymbol{h}_{ul.1}\right|^2 \\ &s.t \quad \boldsymbol{w}_r\boldsymbol{H}_{SI}\boldsymbol{w}_t = 0 \end{aligned} \tag{15}$$

Using similar steps as in [7] the optimal $\boldsymbol{w}_r$can be obtained as

$$\boldsymbol{w}_r^{ZF} = \frac{Dh_{ul,1}^{+}}{Dh_{ul.1}^{+}} \tag{16}$$

Where $\boldsymbol{D} = \boldsymbol{I}_{N_{rx}} - \frac{\boldsymbol{H}_{SI}\boldsymbol{h}_{dl,1}^{\dagger}\boldsymbol{h}_{dl,1}\boldsymbol{H}_{SI}}{\left|\boldsymbol{H}_{SI}\boldsymbol{h}_{dl,1}^{\dagger}\right|}$. Now, substituting $\boldsymbol{w}_r^{ZF}$ and $\boldsymbol{w}_t^{MRT}$ into (1) and (2) we have

$$R_1^{ul} = \log_2\left(1+\frac{p_1\left|\boldsymbol{w}_r^{ZF}\boldsymbol{h}_{ul.1}\right|^2}{p_2\left|\boldsymbol{w}_r^{ZF}\boldsymbol{h}_{ul.2}\right|^2+\sigma_n^2}\right) = \log_2\left(1+\frac{p_1 x_1}{p_2 x_2+\sigma_n^2}\right) \tag{17}$$

$$R_2^{ul} = \log_2\left(1+\frac{p_2\left|\boldsymbol{w}_r^{ZF}\boldsymbol{h}_{ul.2}\right|^2}{\sigma_n^2}\right) = \log_2\left(1+\frac{p_2 x_2}{\sigma_n^2}\right) \tag{18}$$

where $x_1 = |\boldsymbol{w}_r^{ZF}\boldsymbol{h}_{ul.1}|^2$ is a Chi-squared RV with $2N_{rx}$ degrees-of-freedom, denoted by $x_1 \sim \chi^2_{2N_{rx}}$ and $x_2 = |\boldsymbol{w}_r^{ZF}\boldsymbol{h}_{ul.2}|^2$ is an exponential RV, denoted by $x_2 \sim exp(\lambda_{ul,2})$.

4. Performance Analysis

In this section, we characterize the outage probability performance of the system with proposed ZF-based beamforming designs at the FD BS. Outage probability is a key performance metric of the wireless systems which is defined as the probability that the user cannot achieve the target SINR.

4-1 Uplink Performance Analysis

In this subsection, we investigate the outage performance of the NOMA uplink users. For NOMA near user, an outage occurs when the BS cannot detect x_2 and therefore cannot cancel it. Mathematically, the outage probability of the NOMA near user can be written as

$$P_{out,1}^{ul} = 1 - \Pr\left(E_U^1\right) = 1 - \Pr\left(R_1^{ul,i} > R_1^U\right) \tag{19}$$

where $i \in \{TZF, RZF\}$ and R_1^U is the rate threshold for UL transmission of the NOMA near user. Now we present the outage probability result for the NOMA near and far user according to fixed beamforming designs.

Theorem 1: With TZF beamforming design, the UL outage probability of the near UL user is given by

$$P_{out,1}^{ul,TZF} = 1 - \frac{\exp\left(1_{ul,2}\sigma_n^2 + \frac{1_{ul,2}}{\varphi p_2}\right) E_1\left(\frac{\lambda_{ul,2}\left(\varphi\sigma_n^2 + 1\right)}{\varphi p_2}\right)}{\varphi p_2} \tag{20}$$

where, $\varphi = \frac{\gamma_1^U}{p_1}$ and $\gamma_1^U = 2^{R_1^U} - 1$ and $E_1(.)$ denotes the the exponential-integral function of the first order [28], Eq. (8.211.1)].

Proof: To derive the outage probability of the near UL user, by substituting (13) into (19), we have

$$\begin{aligned} P_{out,1}^{ul.TZF} &= 1 - P_r\left(\log_2\left(1 + \frac{p_1 y_1}{p_2 y_2 + \delta_n^2}\right) > R_1^U\right) \\ &= 1 - P_r\left(\frac{p_1 y_1}{p_2 y_2 + \sigma_n^2} > y_1^U\right) \\ &= P_r(y_1 < \varphi(p_2 y_2 + \delta_n^2)) \end{aligned} \tag{21}$$

By invoking the order statistic, $P_{out,1}^{ul,TZF}$ can be expressed as

$$P_{out,1}^{ul,TZF} = \int_0^\infty F_{y_1}\left(\varphi\left(p_2 y + \sigma_n\right)\right) f_{y_2}(y)\, dy \tag{22}$$

By substituting $F_{y_1}(y) = \frac{y}{y+1}$ into (22), and noticing that y_2 is an exponential RV, we have

$$P_{out,1}^{ul,TZF} = \int_0^\infty \frac{\varphi\left(p_2 y + \sigma_n^2\right)}{1 + \varphi\left(p_2 y + \sigma_n^2\right)} \exp\left(-\lambda_{ul,2} y\right) dy \tag{23}$$

To this end, by using the integral identity [26, Eq. (3.353.5)], after some manipulations, the desired result (20) is obtained. We now provide outage probability for far user and for ZF-based beamforming designs.
Theorem 2: The UL outage probability of a far UL user based on TZF scheme is given as

$$P_{out,2}^{ul,TZF} = \left(1 - \exp\left(-\lambda_{ul,2}\xi\right)\right)\left(1 - \frac{\exp\left(\lambda_{ul,2}\sigma_n^2 + \frac{1_{ul,2}}{\varphi p_2}\right) E_1\left(\frac{\lambda_{ul,2}\left(\varphi\sigma_n^2 + 1\right)}{\varphi p_2}\right)}{\varphi p_2}\right) \tag{24}$$

where $\xi = \frac{\gamma_2^U}{\sigma_n^2}$ and $\gamma_i^U = 2^{R_i^U} - 1$.

Proof: At the far user, an outage happens if one of the following events be accomplished: 1) E_U^1: when FD BS cannot decode x_2, 2) E_U^2: when FD BS x_1 cannot discover and therefore cannot cancel it. Due to independent E_U^1 and E_U^2, we have

$$P_{out,2}^{ul} = 1 - \Pr\left(E_U^1 \cap E_U^2\right) = 1 - \Pr\left(E_U^1\right)\Pr\left(E_U^2\right) \tag{25}$$

where $i \in \{TZF, RZF\}$.

By substituting (13) and (17) into (24), the outage probability of the far user based on TZF scheme can be calculated as

$$\boldsymbol{P}_{out.2}^{ul.TZF} = 1 - P_r\left(\frac{p_1 y_1}{p_2 y_2 + \delta_n^2} > \gamma_2^U\right) P_r\left(\frac{p_2 y_2}{\sigma_n^2} > \gamma_2^U\right) = P_r\left(y_1 < \varphi\left(p_2 y_2 + \sigma_n^2\right)\right) P_r\left(y_2 < \xi\right) \tag{26}$$

where $y_1 \sim \chi_{2N}^2$, $y_2 \sim exp(\lambda_{ul,2})$ .Therefore, $P_{out,2}^{ul,TZF}$ is given by

$$P_{out,2}^{ul,TZF} = \left(1 - \exp\left(-1_{ul,2}\,\xi\right)\right)\int_0^\infty F_{y_1}\left(\varphi\left(p_2 y_2 + \sigma_n^2\right)\right) f_{y_2}\left(y\right) dy = \left(1 - \exp\left(-\lambda_{ul,2}\xi\right)\right)\int_0^\infty \frac{\varphi\left(p_2 y + \sigma_n^2\right)}{1 + \varphi\left(p_2 y + \sigma_n^2\right)} \exp\left(-\lambda_{ul,2} y\right) dy \tag{27}$$

To this end, by using the integral identity [26, Eq. (3.353.5)], after some manipulations, the desired result (24) is obtained.

Theorem 3: The UL outage probability of a near UL user based on RZF scheme can be calculated as

$$P_{out,1}^{ul,RZF} = \int_0^\infty \left(\frac{\varphi\left(p_2 x + \sigma_n^2\right)}{1 + \varphi\left(p_2 x + \sigma_n^2\right)}\right)^{N_{rx}-1} \exp\left(-\lambda_{ul,2} x\right) dy \tag{28}$$

Proof: According to RZF beamforming scheme by using (16), (17), where $x_1 \sim \chi_{2(N_{rx}-1)}^2$ and $x_2 \sim exp(\lambda_{ul,2})$. Moreover, $F_{x_1}(x) = \left(\frac{1+x}{x}\right)^{Nrx-1}$. Therefore, $P_{out,1}^{ul,RZF}$ is given by

$$P_{out,1}^{ul,RZF} = \int_0^\infty F_{x_1}\left(\varphi\left(p_2 x + \sigma_n\right)\right) f_{x_2}\left(x\right) dx \tag{29}$$

Then, by substituting the cdf and pdf of x_1, x_2, into (30), we arrive at the desired result in (29).

Theorem 4: The UL outage probability of a far UL user based on RZF scheme is given by

$$P_{out,2}^{ul,RZF} = \left(1 - \exp\left(-\lambda_{ul,2}\xi\right)\right)\int_0^\infty F_{x_1}\left(\varphi\left(p_2 x + \sigma_n^2\right)\right) f_{x_2}\left(x\right) dx = \left(1 - \exp\left(-\lambda_{ul,2}\xi\right)\right)\int_0^\infty \left(\frac{\varphi\left(p_2 x + \sigma_n^2\right)}{1 + \varphi\left(p_2 x + \sigma_n^2\right)}\right)^{N_{rx}-1} \exp\left(-\lambda_{ul,2} x\right) dx \tag{30}$$

Proof: The proof is similar to that of the Theorem 2, and thus omitted.

4-2 Downlink Performance Analysis

In this subsection, we analyze the outage performance of NOMA downlink users. At the near user, an outage happens if one of the following events be accomplished: 1) E_D^1: when D_1cannot detect x_2 and therefore cannot cancel it, 2) E_D^2: when D_1 can discover x_2 but cannot decode x_1.

$$P_{dl,1}^{out} = 1 - \Pr\left(E_D^1 \cap E_D^2\right) = 1 - \Pr\left(R_1^{dl,i} > R_1^D, R_{2\to1}^{dl,i} > R_2^D\right) \quad (31)$$

where $i \in \{TZF, RZF\}$, R_1^D, R_2^D are the rate threshold for DL transmission.

In what follows, we analyze the outage probability for near and far DL user according to fixed beamforming designs.

Theorem 5: The outage probability of near DL user with TZF scheme is given by

$$P_{dl,1}^{out,TZF} = \int_0^\infty \frac{\zeta\left(z+\sigma_n^2\right)^2}{1+\zeta\left(z+\sigma_n^2\right)^2} \times p^2 \exp(-pz)\, dz \quad (32)$$

where $p_1 = p_2 = p_u$ and $\zeta = max\left(\frac{\gamma_1^D}{c_1}, \frac{\gamma_2^D}{c_2 - c_1\gamma_2^D}\right)$ with $c_1 = p_b a_1$, $c_2 = p_b a_2$, and $\gamma_i^D = 2^{R_i^D} - 1$.

Proof: By substituting w_t^{ZF} into (3), (5) $R_1^{TZF}, R_{2\to1}^{TZF}$ can be obtained, respectively. Therefore, the outage probability of D_1 can be calculated as

$$\begin{aligned} P_{dl,1}^{out,TZF} &= 1 - P_r\left(\log\left(1+\frac{p_b a_1 \left|\boldsymbol{h}_{dl,1}\boldsymbol{w}_t^{ZF}\right|^2}{I_{dl,1}+\sigma_n^2}\right) > R_1^D, \log\left(1+\frac{p_b a_2 \left|\boldsymbol{h}_{dl,1}\boldsymbol{w}_t^{ZF}\right|^2}{p_b a_1 \left|\boldsymbol{h}_{dl,1}\boldsymbol{w}_t^{ZF}\right|^2 + I_{dl,1}+\sigma_n^2}\right) > R_2^D \right. \\ &= 1 - \Pr\left(\frac{c_1\vartheta_1}{I_{dl,1}+\sigma_n^2} > \gamma_1^D, \frac{c_2\vartheta_1}{c_1 Y_1 + I_{dl,1}+\sigma_n^2} > \gamma_2^D\right) \\ &= 1 - \Pr\left(\frac{c_1}{\gamma_1^D}\vartheta_1 > I_{dl,1}+\sigma_n^2, \frac{\left(c_2 - c_1\gamma_2^D\right)}{\gamma_2^D}\vartheta_1 > I_{dl,1}+\sigma_n^2\right) \\ &= \Pr\left(\vartheta_1 < \zeta\left(I_{dl,1}+\sigma_n^2\right)\right) \end{aligned} \quad (33)$$

where $\vartheta_1 = \left|\boldsymbol{h}_{dl,1}\boldsymbol{w}_t^{ZF}\right|^2$. We note that, $P_{dl,1}^{out,TZF} = 1$ when $\gamma_2^D > \frac{c_2}{c_1}$. On the other hand, for $0 < \gamma_2^D < \frac{c_2}{c_1}$ by using the order static, $P_{dl,1}^{out,TZF}$ is given by

$$P_{dl,1}^{out,TZF} = \int_0^\infty F_{\vartheta_1}\left(\zeta\left(I_{dl,1}+\sigma_n\right)\right) f_{I_{dl,1}}(\vartheta)\, d\vartheta \quad (34)$$

Moreover, the pdf of $I_{dl,1} = Z_1 + Z_2$, where $Z_1 \sim exp\left(p_1\lambda_{h_{11}}\right)$ and $Z_2 \sim exp\left(p_2\lambda_{h_{21}}\right)$. Therefore, the pdf of $I_{dl,1}$can be defined as

$$f_{I_{dl,1}}(z) = \begin{cases} \frac{p_1\lambda_{h_{11}} p_2\lambda_{h_{12}}}{p_2\lambda_{h_{12}} - p_1\lambda_{h_{11}}}\left(e^{-p_1\lambda_{h_{11}}z} - e^{-p_2\lambda_{h_{12}}z}\right) & p_1\lambda_{h_{11}} \neq p_2\lambda_{h_{12}} \\ p^2\lambda^2 z e^{-p\lambda z} & p_1\lambda_{h_{11}} = p_2\lambda_{h_{12}} = p\lambda \end{cases} \quad (35)$$

Therefore, for $\lambda_{h_{11}} = \lambda_{h_{21}} = 1$ and $p_1 = p_2 = p$, thus by substituting (36) into (35), we obtained (33).

Theorem 6: The outage probability of far DL user based on TZF scheme is given by

where $b_1 = p_b a_1$and $b_2 = p_b a_2$.

$$P_{dl,2}^{out,TZF}=\begin{cases}\int_0^{\infty}\left(\dfrac{\gamma_2^D\left(y+\sigma_n^2\right)}{\gamma_2^D\left(y+\sigma_n^2\right)+b_2-\gamma_2^D b_1}\right)^{N_t-1} p^2e^{-py}dy & 0<\gamma_2^D<\dfrac{b_2}{b_1}\\ 1 & \gamma_2^D>\dfrac{b_2}{b_1}\end{cases} \tag{36}$$

Proof: The DL outage probability of a far user occurs when D_2 cannot decode x_2. Therefore, the outage probability of D_2 is defined as

$$\begin{aligned}P_{dl,2}^{out,i}&=1-\Pr\left(E_D^1\right)\\&=\Pr\left(R_2^{dl,i}<R_2^D\right)\end{aligned} \tag{37}$$

where $i\in\{TZF,RZF\}$. According to (37), we need to calculate $F_{\gamma_2^{dl,TZF}}(\tau)$, which can be expressed as

$$\begin{aligned}F_{\gamma_2^{dl,TZF}}(\tau)&=\Pr\left(\frac{b_2\vartheta_2}{b_1\vartheta_2+I_{dl,2}+\sigma_n^2}<\tau\right)\\&=\Pr\left(\left(b_2-\tau b_1\right)\vartheta_2<\tau\left(I_{dl,2}+\sigma_n^2\right)\middle| I_{dl,2}\right)\\&\begin{cases}\int_0^{\infty}F_{\vartheta_2}\left(\dfrac{\tau\left(I_{dl,2}+\sigma_n^2\right)}{b_2-zb_1}\right)f_{I_{dl,2}}(x)dx & 0<\tau<\dfrac{b_2}{b_1}\\ 1-\int_0^{\infty}F_{\vartheta_2}\left(\dfrac{\tau\left(I_{dl,2}+\sigma_n^2\right)}{b_2-\tau b_1}\right)f_{I_{dl,2}}(x)dx & \tau>\dfrac{b_2}{b_1}\end{cases}\end{aligned} \tag{38}$$

where $\vartheta_2\sim\chi^2_{2(N_t-1)}$, $I_{dl,2}=X_1+X_2$ where $X_1\sim exp(p_1\lambda_{h_{21}})$ and $X_2\sim exp(p_1\lambda_{h_{22}})$. Therefore, $f_{I_{dl,2}}(x)$ is given in (35). Thus, $F_{\gamma_2}(\tau)$ is given by

$$F_{\gamma_2^{dl,TZF}}(\tau)=\begin{cases}\int_0^{\infty}\left(\dfrac{\tau\left(x+\sigma_n^2\right)}{\tau\left(x+\sigma_n^2\right)+b_2-\tau b_1}\right)^{N_t-1}\times p^2xe^{-xp}dx & 0<\tau<\dfrac{b_2}{b_1}\\ 1 & \tau>\dfrac{b_2}{b_1}\end{cases} \tag{39}$$

To this end, $P_{dl,2}^{out,TZF}$ is obtained as $P_{dl,2}^{out,TZF}=F_{\gamma_2^{dl,TZF}}(\gamma_2^D)$.

Theorem 7: The outage probability of near DL user based on RZF scheme is given by

$$P_{dl,1}^{out,RZF}=\int_0^{\infty}\frac{\zeta\left(z+\sigma_n^2\right)^2}{1+\zeta\left(z+\sigma_n^2\right)^2}\times p^2\exp\left(-pz\right)dz \tag{40}$$

Theorem 8: The outage probability of far DL user based on TZF scheme is given by

$$P_{dl,2}^{out,RZF}=\begin{cases}\int_0^{\infty}\left(\dfrac{\gamma_2^D\left(y+\sigma_n^2\right)}{\gamma_2^D\left(y+\sigma_n^2\right)+b_2-\gamma_2^D b_1}\right)^{N_t} p^2e^{-py}dy & 0<\gamma_2^D<\dfrac{b_2}{b_1}\\ 1 & \gamma_2^D>\dfrac{b_2}{b_1}\end{cases} \tag{41}$$

Proof: The proof is similar to that of the Theorem ۷, and thus omitted.

5. Numerical Results

In this section, we present numerical results to validate the accuracy and efficiency of the proposed beamforming designs. Unless otherwise stated, in all simulations the value of the network parameters are set as $a_1 = 0.1$, $a_2 = 0.9$, $\lambda_{h_{dl,1}} = 0.75$, $\lambda_{h_{dl,2}} = 0.5$, $\lambda_{h_{ul,1}} = 0.75$, $\lambda_{h_{ul,2}} = 0.5$, and $\sigma_n^2 = 1$. In our simulations, we further include the performance of the MRC/MRT beamforming design as a baseline for comparison where $\boldsymbol{w}_t$ and $\boldsymbol{w}_r$ are matched to the links corresponding to the near DL and UL users, respectively.

Fig. 2 shows the effect of BS transmit power, p_b , on the outage probability of the near DL user with TZF and RZF beamforming schemes, and for different antenna configurations at the BS. In this example, in order to study the impact of the antenna configuration on the outage performance of the system, the total number of transmit and receive antennas is kept the same for different scenarios. Firstly, it can be observed that the analytical results match the simulation results. Moreover, for different antenna configurations at the BS, the TZF scheme outperforms the RZF scheme, while the gap between the RZF and TZF scheme is increased when the number of transmit antennas at the BS is increased. Moreover, it can be observed that by increasing the number of transmitting antennas at the BS, the outage probability of the near DL user is significantly improved. In other words, by increasing the number of the transmit antennas at the BS, the diversity order of the system is improved. This is intuitive, because by increasing the number of transmit antennas at the BS, the number of degrees-of-freedom at the BS for the ZF-based beamforming is increased and accordingly the outage performance of the system is improved.

In Fig. 3 we compare the outage performance of D_2 with different beamforming designs and for different antenna configurations at the BS. For this example, we set $R_1^D = R_2^D = 0.5bps/Hz$, and $p_1 = p_2 = 15dBm$ and the total number of antennas at the BS is 6. From this figure, we observe that the TZF scheme outperforms the RZF scheme at low transmit power regime. However, at the middle-to-high transmit power regime, TZF scheme provides much better outage performance at D_2 . Moreover, by increasing the number of transmit and receive antennas at the BS, the diversity order achieved by the RZF scheme remains constant, while the diversity order of the TZF scheme is increased. More specifically when the number of transmit antennas at the BS is increased, regardless the number of receiving antennas at the BS, the coding gain achieved by the RZF scheme is slightly improved, while the diversity gain of the system remains constant. Finally, by considering the results of figure 1 and 2, we observe that by applying the RZF scheme at the BS, while deploying the same number of antennas at the BS, the performance of both near and far DL users can be significantly improved comparing with the TZF scheme.

Fig. 4 investigates the UL outage probability of the NOMA near user as a function of p_1 and for two different values of the BS transmit power and for different antenna configurations. In Fig. 4a, by increasing the transmit power of the UL near user, the outage performance of U_1 is improved. This improvement is more pronounced by increasing the number of receiving antennas at the BS and deploying the RZF scheme. From Fig 4b, we observe that by decreasing the transmit power of U_2 and increasing the number of transmit antennas with respect to the number of receive antennas the outage probability of U_1 is improved for both TZF and RZF schemes. Comparing TZF and RZF schemes for the same antenna configuration, we find that the TZF scheme delivers better outage probability than the RZF scheme.

Fig. 5 shows the UL outage probability for the NOMA far user as a function of p_1 and for different antenna configurations. In this example we set, $p_2 = 15dBm$ and $p_b = 45dBm$ and total number of antennas at the BS is 6. From this figure, we observe that both RZF and TZF schemes provide the same diversity order, which is significantly improved increasing the number of transmit antenna. Moreover, we observe that RZF scheme outperforms the TZF scheme in terms of coding gain and the gap between the two schemes is increased when the number of transmit antennas is more than the receive antennas.

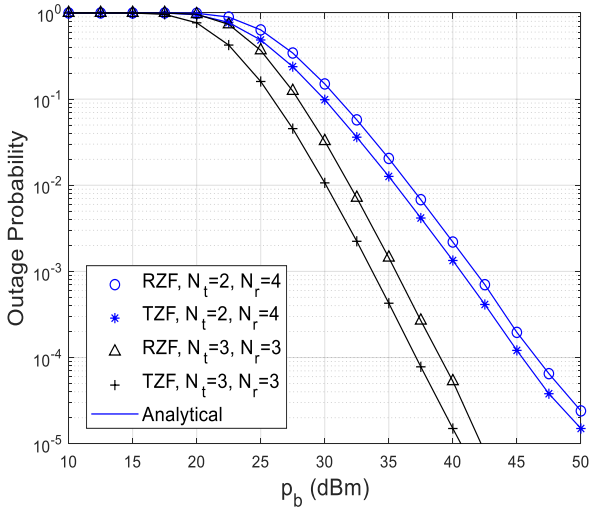

Figure 2. Outage Probability of D_1 versus p_b $(R_1 = R_2 = 0.5bps/Hz, p_1 = p_2 = 15dBm)$.

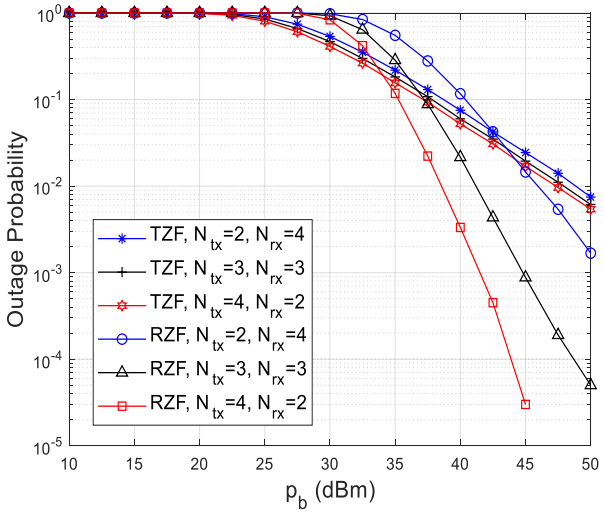

Figure 3. Outage Probability of D_2 versus p_b $(R_1^D = R_2^D = 0.5bps/Hz, p_1 = p_2 = 15dB)$.

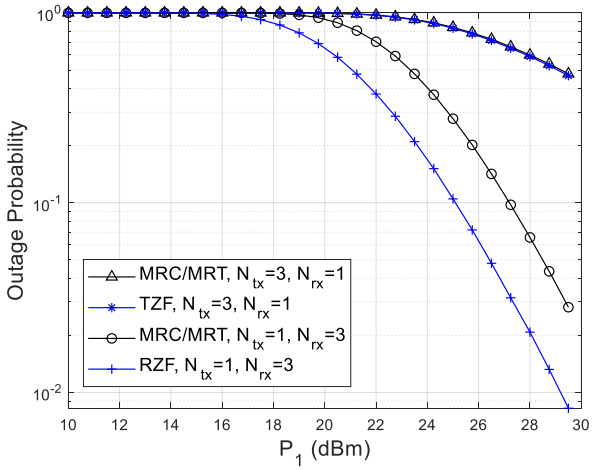

Figure 4a. Outage Probability of U_1 versus p_1 $(p_2 = 25dBm, p_b = 45dBm, R_1^U = R_2^U = 0.5bps/Hz)$.

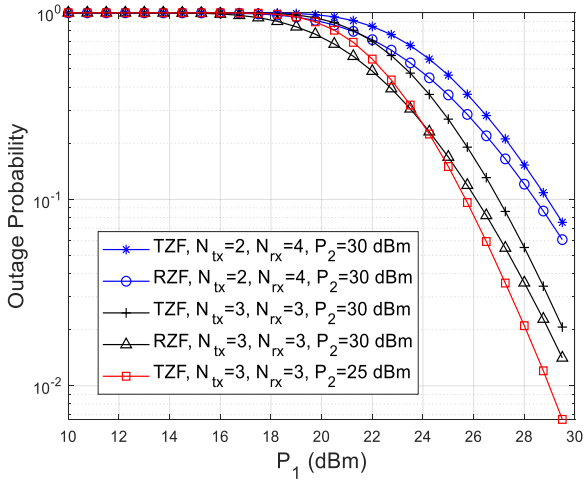

Figure 4b. Outage Probability of U_1 versus p_1 ($p_b = 45dBm, R_1^U = R_2^U = 0.5bps/Hz$).

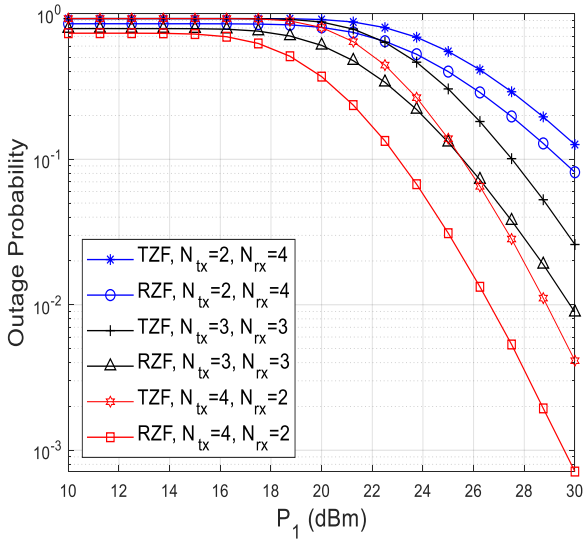

Figure 5. Outage Probability of U_2 versus p_1 ($p_2 = 15dBm, p_b = 45dBm$).

6. Conclusion

We investigated the outage performance of a FD-enable cellular system with NOMA, where a pair of UL and DL users simultaneously communicate with the multi-antenna FD BS. We applied the ZF-based beamforming design at the BS to mitigate the SI, while MRT and MRC designs applied to the BS to improve the received SINR at the DL users and BS, respectively. Closed-form results have been derived for the outage probability of the UL and DL NOMA users. Our results provide a framework to study the impact of different system parameters, including the antenna configuration at the BS and the power transmit level at the BS and users, on the performance of the system.

References

[1] Z. Zhang, X. Chai, K. Long, A. V. Vasilakos and L. Hanzo, "Full duplex techniques for 5G networks: self-interference cancellation, protocol design, and relay selection," in *IEEE Communications Magazine*, vol. 53, no. 5, pp. 128-137, May 2015, doi: 10.1109/MCOM.2015.7105651.

[2] Z. Ding, X. Lei, G. K. Karagiannidis, R. Schober, J. Yuan and V. K. Bhargava, "A Survey on Non-Orthogonal Multiple Access for 5G Networks: Research Challenges and Future Trends," in *IEEE Journal on Selected Areas in Communications*, vol. 35, no. 10, pp. 2181-2195, Oct. 2017, doi: 10.1109/JSAC.2017.2725519.

[3] M. Mohammadi *et al.*, "Full-Duplex Non-Orthogonal Multiple Access for Next Generation Wireless

Systems," in *IEEE Communications Magazine*, vol. 57, no. 5, pp. 110-116, May 2019, doi: 10.1109/MCOM.2019.1800578.

[4] A.Sabharwal, P. Schniter, D. Guo, D. W. Bliss, S. Rangarajan and R. Wichman, "In-Band Full-Duplex Wireless: Challenges and Opportunities," in *IEEE Journal on Selected Areas in Communications*, vol. 32, no. 9, pp. 1637-1652, Sept. 2014, doi: 10.1109/JSAC.2014.2330193.

[5] M. Duarte, C. Dick and A. Sabharwal, "Experiment-Driven Characterization of Full-Duplex Wireless Systems," in *IEEE Transactions on Wireless Communications*, vol. 11, no. 12, pp. 4296-4307, December 2012, doi: 10.1109/TWC.2012.102612.111278.

[6] J. Lee and T. Q. S. Quek, "Hybrid Full-/Half-Duplex System Analysis in Heterogeneous Wireless Networks," in *IEEE Transactions on Wireless Communications*, vol. 14, no. 5, pp. 2883-2895, May 2015, doi: 10.1109/TWC.2015.2396066.

[7] M. Mohammadi, B. K. Chalise, H. A. Suraweera, C. Zhong, G. Zheng and I. Krikidis, "Throughput Analysis and Optimization of Wireless-Powered Multiple Antenna Full-Duplex Relay Systems," in *IEEE Transactions on Communications*, vol. 64, no. 4, pp. 1769-1785, April 2016, doi: 10.1109/TCOMM.2016.2527785.

[8] M. Amjad, F. Akhtar, M. H. Rehmani, M. Reisslein and T. Umer, "Full-Duplex Communication in Cognitive Radio Networks: A Survey," in *IEEE Communications Surveys & Tutorials*, vol. 19, no. 4, pp. 2158-2191, Fourthquarter 2017, doi: 10.1109/COMST.2017.2718618.

[9] S. Chinnadurai, P. Selvaprabhu, Y. Jeong, A.L. Sarker, H. Hai, W. Duan, et al. "User clustering and robust beamforming design in multicell MIMO-NOMA system for 5G communications," *AEU-Int J Electron Commun*, vol:78,pp. 181-191, 2017,doi:10.1016/j.aeue.2017.05.021.

[10] Mobini Z. Secrecy performance of non-orthogonal multiple access cognitive untrusted relaying with friendly jamming. *AEU-Int J Electron Commun* ,vol:118,p. 153156 ,2020,doi:10.1016/j.aeue.2020.153156.

[11] J. Zhu, J. Wang, Y. Huang, K. Navaie, Z. Ding and L. Yang, "On Optimal Beamforming Design for Downlink MISO NOMA Systems," in *IEEE Transactions on Vehicular Technology*, vol. 69, no. 3, pp. 3008-3020, March 2020, doi: 10.1109/TVT.2020.2966629.

[12] C. Zhong and Z. Zhang, "Non-Orthogonal Multiple Access With Cooperative Full-Duplex Relaying," in *IEEE Communications Letters*, vol. 20, no. 12, pp. 2478-2481, Dec. 2016, doi: 10.1109/LCOMM.2016.2611500.

[13] A.Tregancini, E. E. B. Olivo, D. P. M. Osorio, C. H. M. de Lima and H. Alves, "Performance Analysis of Full-Duplex Relay-Aided NOMA Systems Using Partial Relay Selection," in *IEEE Transactions on Vehicular Technology*, vol. 69, no. 1, pp. 622-635, Jan. 2020, doi: 10.1109/TVT.2019.2952526.

[14] M. Mohammadi, B. K. Chalise, A. Hakimi, Z. Mobini, H. A. Suraweera and Z. Ding, "Beamforming Design and Power Allocation for Full-Duplex Non-Orthogonal Multiple Access Cognitive Relaying," in *IEEE Transactions on Communications*, vol. 66, no. 12, pp. 5952-5965, Dec. 2018, doi: 10.1109/TCOMM.2018.2858811.

[15] X. Wang, M. Jia, Q. Guo, I. W. Ho and F. C. Lau, "Full-Duplex Relaying Cognitive Radio Network With Cooperative Nonorthogonal Multiple Access," in *IEEE Systems Journal*, vol. 13, no. 4, pp. 3897-3908, Dec. 2019, doi: 10.1109/JSYST.2019.2927509.

[16] H. V. Nguyen, V. Nguyen, O. A. Dobre, D. N. Nguyen, E. Dutkiewicz and O. Shin, "Joint Power Control and User Association for NOMA-Based Full-Duplex Systems," in *IEEE Transactions on Communications*, vol. 67, no. 11, pp. 8037-8055, Nov. 2019, doi: 10.1109/TCOMM.2019.2933217.

[17] Y. Sun, D. W. K. Ng, Z. Ding and R. Schober, "Optimal Joint Power and Subcarrier Allocation for Full-Duplex Multicarrier Non-Orthogonal Multiple Access Systems," in *IEEE Transactions on Communications*, vol. 65, no. 3, pp. 1077-1091, March 2017, doi: 10.1109/TCOMM.2017.2650992.

[18] Z. Mobini, M. Mohammadi, B. K. Chalise, H. A. Suraweera and Z. Ding, "Beamforming Design and Performance Analysis of Full-Duplex Cooperative NOMA Systems," in *IEEE Transactions on Wireless Communications*, vol. 18, no. 6, pp. 3295-3311, June 2019, doi: 10.1109/TWC.2019.2913425.

[19] Y. Liu, Z. Ding, M. Elkashlan and H. V. Poor, "Cooperative Non-orthogonal Multiple Access With Simultaneous Wireless Information and Power Transfer," in *IEEE Journal on Selected Areas in Communications*, vol. 34, no. 4, pp. 938-953, April 2016, doi: 10.1109/JSAC.2016.2549378.

[20] Z. Wei, L. Yang, D. W. K. Ng, J. Yuan and L. Hanzo, "On the Performance Gain of NOMA Over OMA in Uplink Communication Systems," in *IEEE Transactions on Communications*, vol. 68, no. 1, pp. 536-568, Jan. 2020, doi: 10.1109/TCOMM.2019.2948343.

[21] Z. Ding, P. Fan and H. V. Poor, "On the Coexistence Between Full-Duplex and NOMA," in *IEEE Wireless Communications Letters*, vol. 7, no. 5, pp. 692-695, Oct. 2018, doi: 10.1109/LWC.2018.2811492.

[22] A.Memarinejad, M. Mohammadi, and M.B. Tavakoli. "Full-duplex NOMA cellular networks: Beamforming design and user scheduling," *AEU-International Journal of Electronics and Communications* ,vol.126, p. 153415,2020, doi:10.1016/j.aeue.2020.153415.

[23] Z. Ding, P. Fan and H. V. Poor, "Impact of User Pairing on 5G Nonorthogonal Multiple-Access Downlink Transmissions," in *IEEE Transactions on Vehicular Technology*, vol. 65, no. 8, pp. 6010-6023, Aug. 2016 , doi: 10.1109/TVT.2015.2480766..

[24] K. S. Ali, M. Haenggi, H. ElSawy, A. Chaaban and M. Alouini, "Downlink Non-Orthogonal Multiple Access (NOMA) in Poisson Networks," in *IEEE Transactions on Communications*, vol. 67, no. 2, pp. 1613-1628, Feb. 2019, doi: 10.1109/TCOMM.2018.2877328.

[25] G. C. Alexandropoulos, M. Kountouris and I. Atzeni, "User scheduling and optimal power allocation for full-duplex cellular networks," *IEEE International Workshop on Signal Processing Advances in Wireless Communications (SPAWC)*, 2016, pp. 1-6, doi: 10.1109/SPAWC.2016.7536726.

[26] M. S. Ali, H. Tabassum and E. Hossain, "Dynamic User Clustering and Power Allocation for Uplink and Downlink Non-Orthogonal Multiple Access (NOMA) Systems," in *IEEE Access*, vol. 4, pp. 6325-6343, 2016, doi: 10.1109/ACCESS.2016.2604821.

[27] H. A. Suraweera, I. Krikidis, G. Zheng, C. Yuen and P. J. Smith, "Low-Complexity End-to-End Performance Optimization in MIMO Full-Duplex Relay Systems," in *IEEE Transactions on Wireless Communications*, vol. 13, no. 2, pp. 913-927, February 2014, doi: 10.1109/TWC.2013.122313.130608.

[28] S. Gradshteyn and I. M. Ryzhik, Table of Integrals, Series and Products, 7th ed. San Diego, CA, USA: Academic, 2007.